Final Report: Airplane Design Group Project (Group 2)

Sana Noor, Omar Hassan, David Charland, Reuben O' Neill

George Washington University

MAE 6247 - Aircraft Design I

Professor Murray Snyder

April 26, 2023

Table Of Contents

Executive Summary

Designing a cargo plane that focuses on electric propulsion presents unique challenges and opportunities. To overcome these challenges, we have designed our aircraft to incorporate replaceable battery packs located in the fuselage. This design innovation allows the aircraft to operate with reduced emissions, noise, and fuel costs. This forward-thinking design is used to address the challenges of downtime in between flights. Not only will the battery packs help distribute the weight of the aircraft and keep it in balance, but in addition it will also diminish the necessity for the development of charging infrastructure at airports for charging the entirety of the plane, thereby reducing overall cost.

Another design development that supports electrical propulsion are electric motors evenly spaced along the wing of the aircraft to provide uniformly distributed thrust. An aircraft that uses multiple electric motors instead of a single engine for propulsion can offer multiple advantages. These benefits include optimization of the overall performance of the aircraft from the distributed propulsion system. If one engine fails, the aircraft can continue to operate. This precaution enhances the overall safety by minimizing the likelihood of catastrophic engine failure. Lastly, it enhances maneuverability to control roll, pitch, and yaw, increasing control throughout takeoff, cruise, and landing.

Incorporating a propeller on the nose of the aircraft that is optimized for the use of Jet A fuel for cruise flight can significantly improve the overall efficiency and range. The propeller can provide lift and thrust, which improves overall safety because it can enhance the aircraft's level of control during takeoff and landing. Propellers have a higher efficiency when converting fuel into forward motion when the aircraft is flying at low altitudes and slower velocities. The aircraft can therefore achieve higher fuel efficiency, which in turn increases its range. Jet engines are not optimized for low speeds and altitudes; they are more efficient in high speeds and altitudes during cruise flight.

In conclusion, designing a hybrid electric-powered aircraft requires a delicate balance between several factors including range, payload capacity, battery energy density, and cost to name a few. The progress that will be made in material science and battery technology will heavily impact the success of this design.

Model Aircraft Profiles

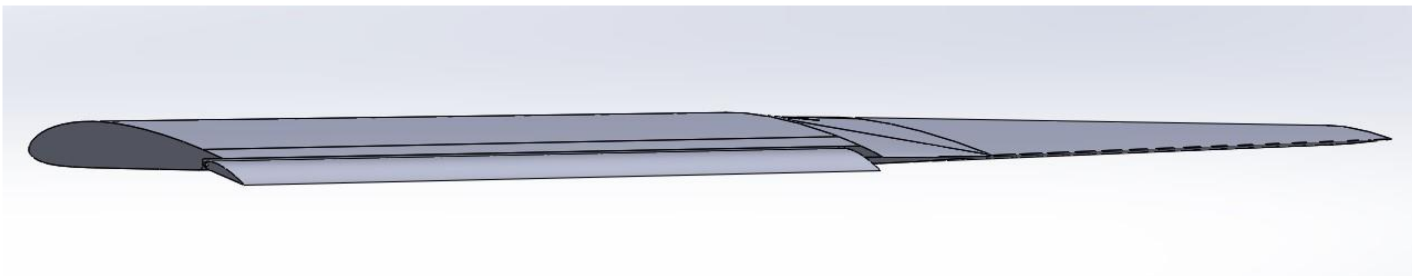

Wing with Flap. **Figure I**

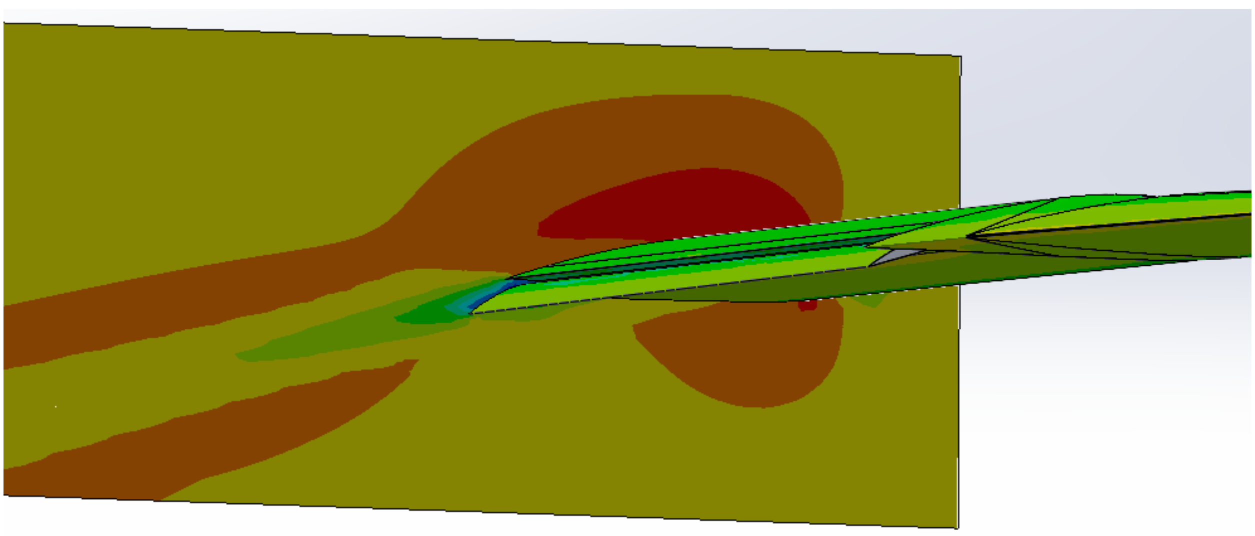

Velocity Cut Plot of Flaps, 15-degree angle. **Figure II**

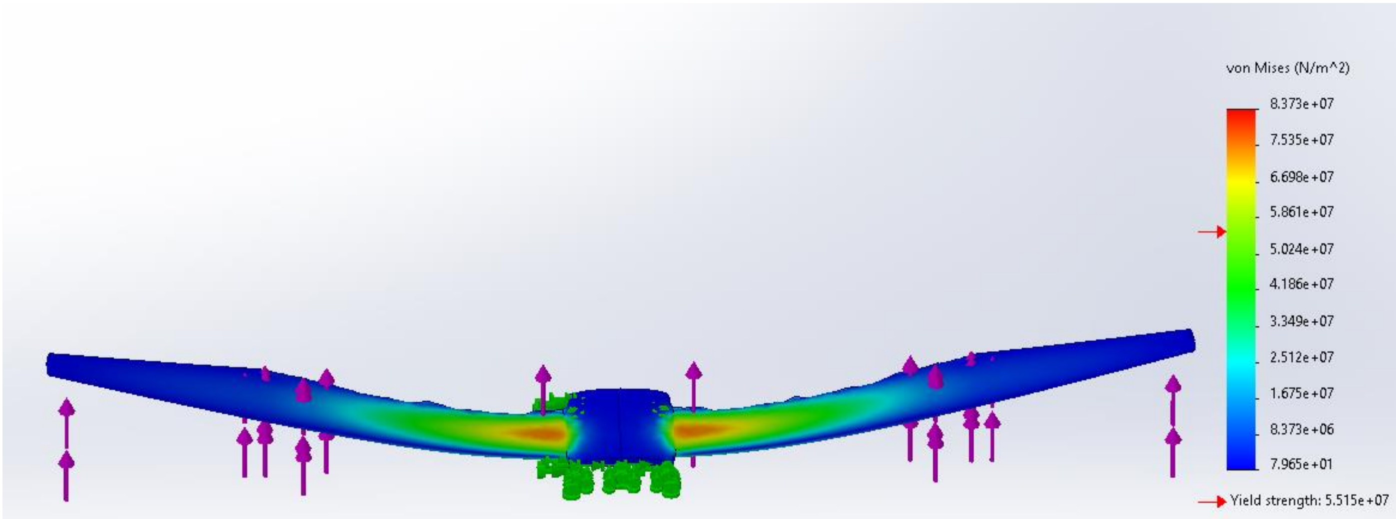

Wing Stress. **Figure III**

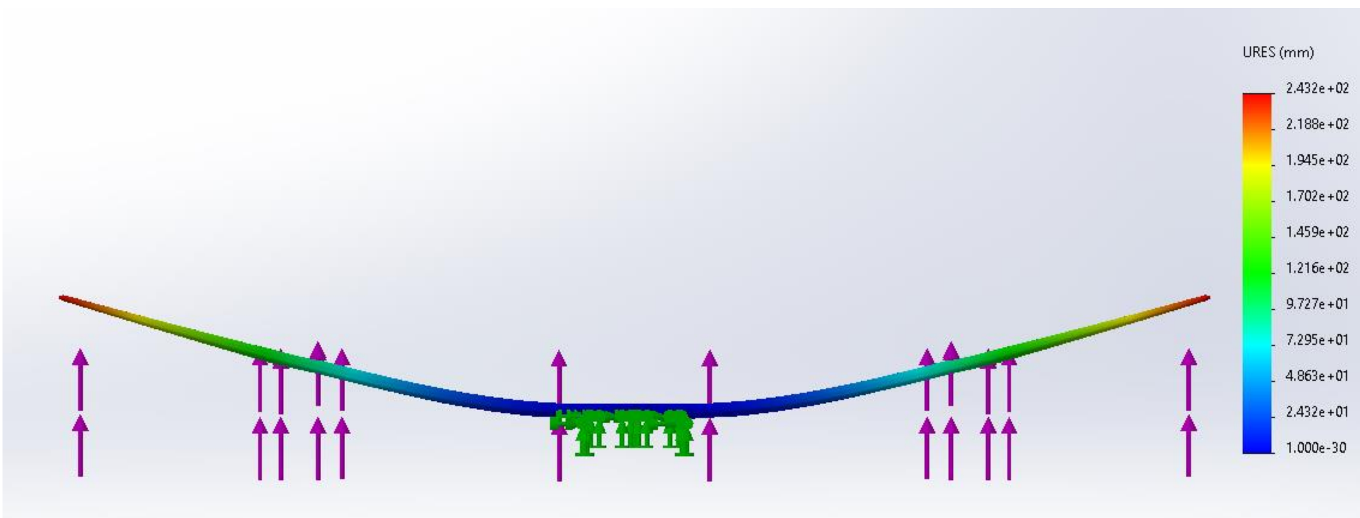

Wing Displacement from lift force. **Figure IV**

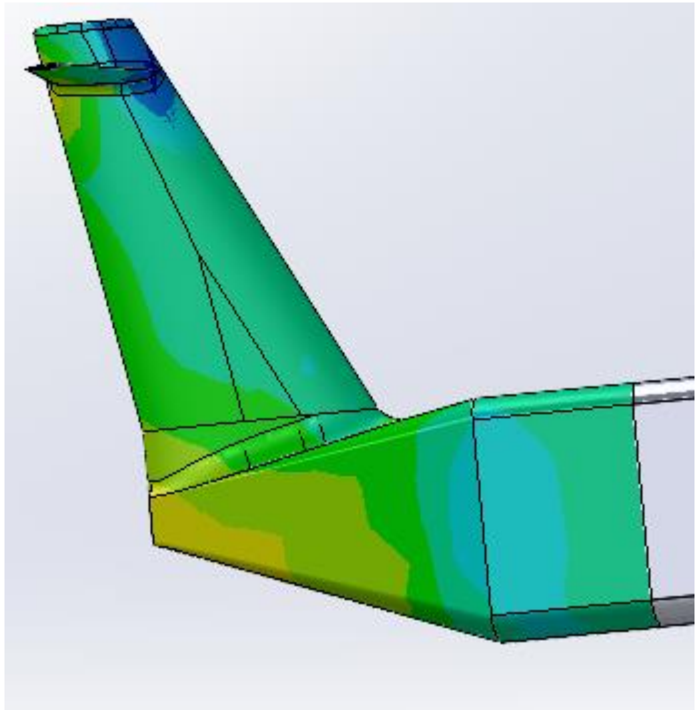

Tail Surface Plot. **Figure V**

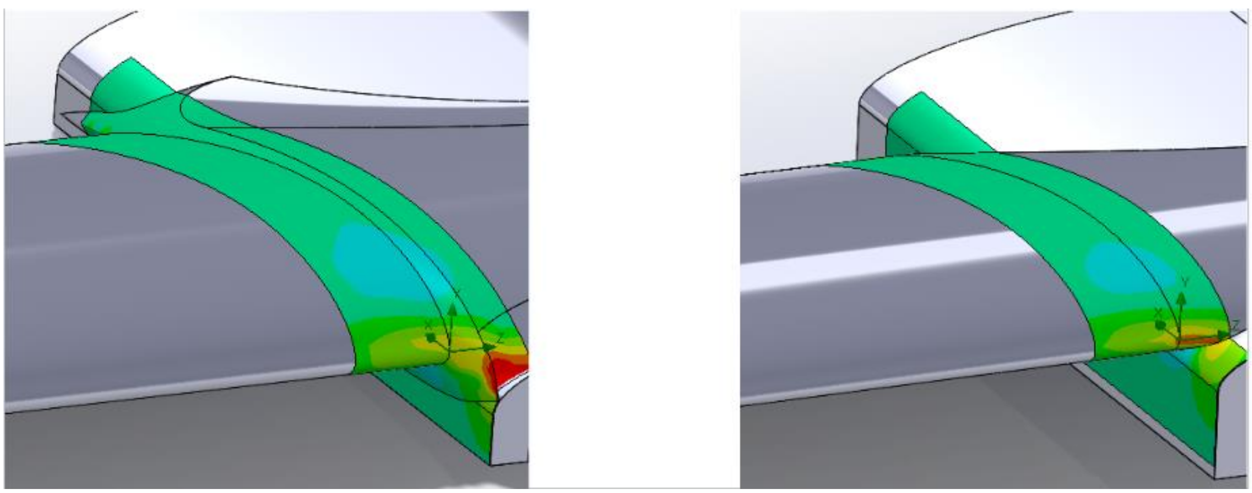

Pressure Comparisons: With & Without Filet Respectively. [Located on wing root]
Figure VI

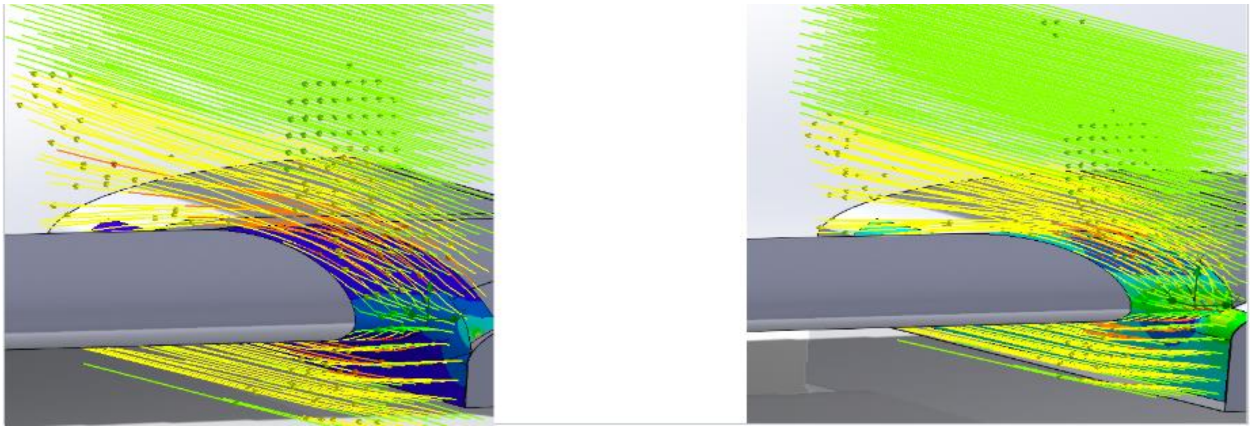

Flow Visualizations: With & Without Filet Respectively. [Located on wing root] **Figure VII**

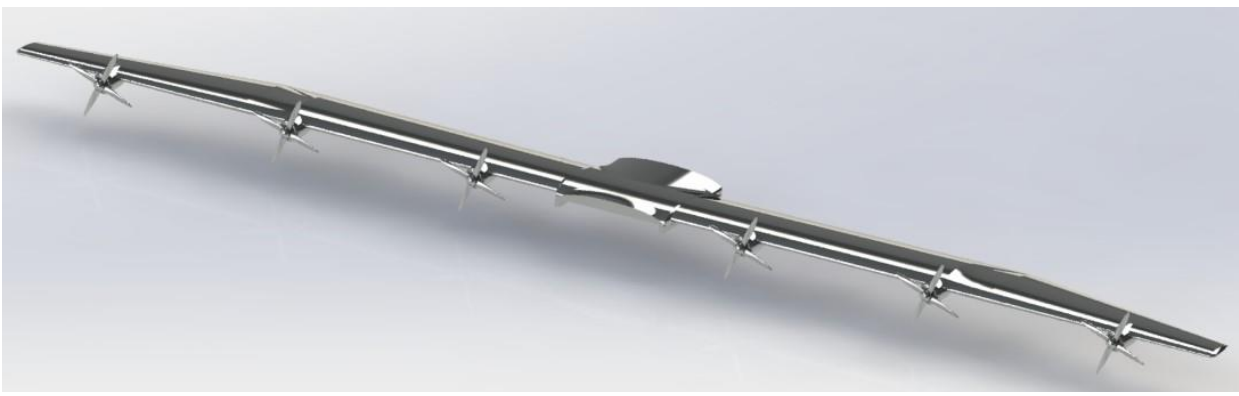

Wing with Electric motors. **Figure VIII**

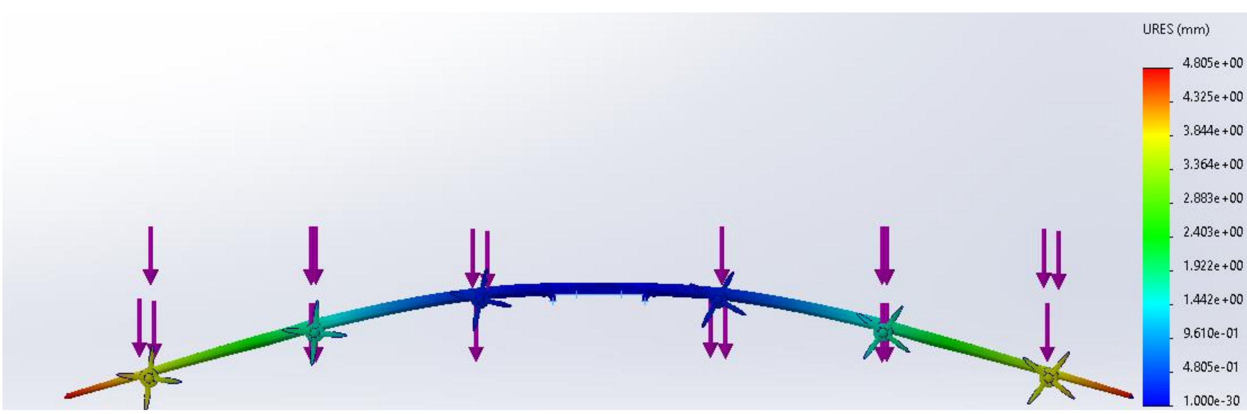

Wing displacement from the motor weight. **Figure IX**

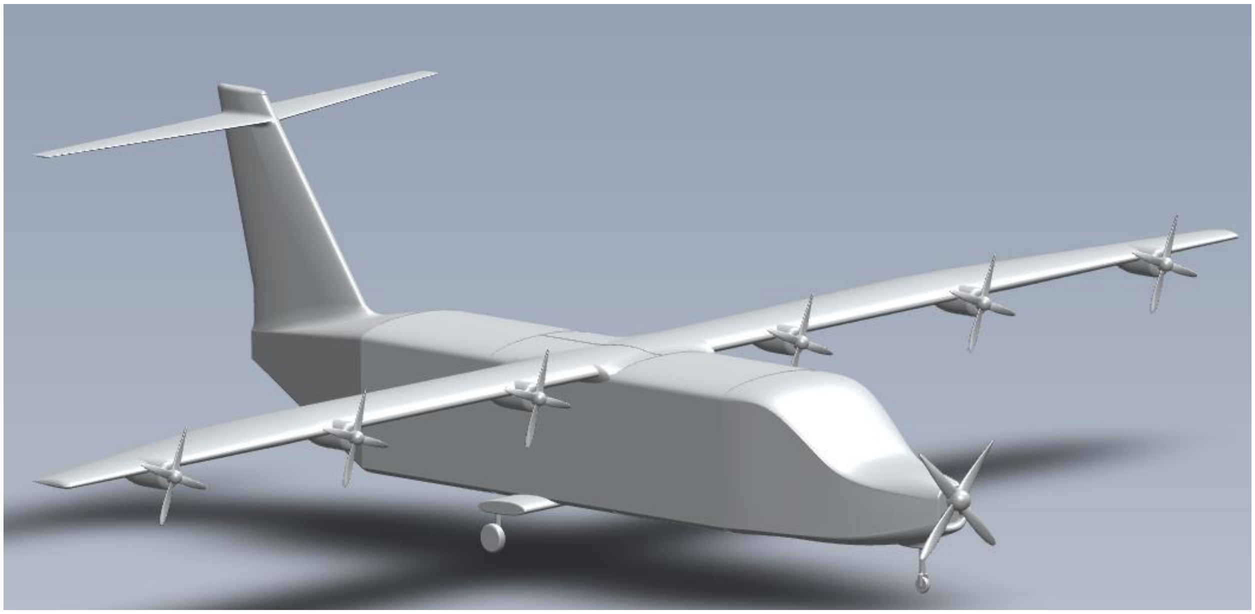

Full plane render. **Figure X**

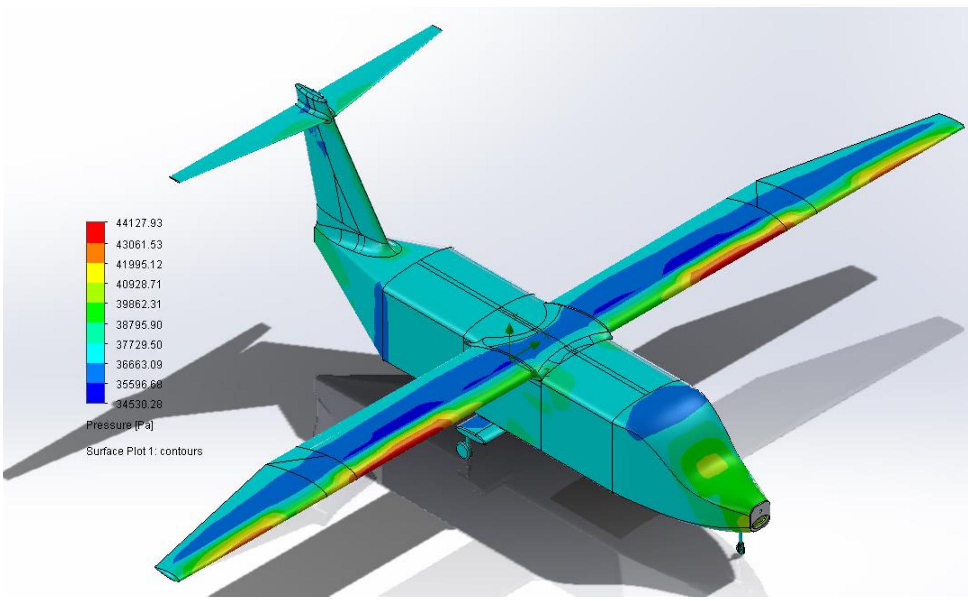

Full plane pressure contour. **Figure XI**

Aircraft Parameters

Max weight	8391.46kg
Wing area	17.05m^2
Span	23.74m
Taper	0.42
Root chord	1.82m
Tip chord	0.76m
Cruise velocity	95.2m/s
Stall velocity	30m/s
Cruise density	0.55kg/m^3
MAC	1.59m
Wing Wetted area	20.14m^2
Cruise lift	83191.66N
Takeoff lift	85573.73N
Drag	2908.87N
L/D	28.61
Cruise altitude	7.62km
Cruise thrust	3729.12N
Propeller diameter	1.5m
Propeller diameter	1m (X6)
Climb thrust	11942.36N
Root-middle airfoil	NACA4415
Middle-tip airfoil	NACA2415

Assumptions & Key Features

Assumptions:

- Propeller efficiency 80%
- Cargo door for similar size and location to Cessna SkyCourrier for ease of loading/unloading
- Cargo bay designed for LD3 containers [61 in x 88 in x 64 in, max weight capacity 3,500 lbs]
- Cl increase for takeoff is 0.78[1]
- Based on the Cd v AoA curve Cd for the airfoils is 0.009[2]

Key Features:

- Replaceable battery packs [located in fuselage]
- Evenly-spaced electric motors along the wings for the purpose of distributed thrust
- Propeller on the nose optimized for cruise using Jet A and SAF mixture

Implementation of Green Technology

The selected method of green technology is a hybrid aircraft. This has been implemented in the form of 6 electric motors along the span of the aircraft, which can be seen in *Figure VIII*. Three motors on each wing will be used solely for the takeoff and climb section of the flight. This is due to the takeoff and climb section of the flight consuming 460 gallons of fuel. By eliminating this portion of the flight, we can reduce carbon emissions by about 22%. We spaced out the motors on the wing for a few reasons, including an even distribution of thrust, reducing the amount of rudder needed on takeoff from asymmetric thrust, and decreasing the amount of wingtip vortices that have the capacity to form. The ENGINeUS™ Aircraft Electric motors were selected for their high power capability, climb max height, and their relatively small engine size. The engine is capable of operating at 3000 rpm if necessary, the capacity to climb up to 8 km is

[1] Raymer, Daniel P. *Aircraft Design: A Conceptual Approach*. American Institute of Aeronautics and Astronautics, 2018.

[2] "Airfoil Plot NACA2415." *NACA 2415 (n2415-IL)*, http://airfoiltools.com/airfoil/details?airfoil=n2415-il.

"Airfoil Plot NACA4415." *NACA 4415 (NACA4415-IL)*, http://airfoiltools.com/airfoil/details?airfoil=naca4415-il.

available, which exceeds the minimum requirement by .4 km, and the size is approximately that of a large cooking pot.[3]

During the cruise portion of the flight, a conventional turboprop engine will be used. A Pratt & Whitney PT6A-11AG turboprop engine was selected to be the power plant for this segment of flight. The horsepower requirement for this application was determined based on the cruise thrust. The PT6 engine series was deemed suitable as it can be sized to the loading specifications of the aircraft. At the altitude at which this aircraft operates, conventional turboprop engines are already a highly efficient choice for the cruise phase of flight and the 11AG model, with its 550 horsepower output[4], should be well-suited for the task. The turboprop will increase efficiency further since it can now be optimized solely for the cruise segment of the flight. Running the engine at higher RPMs results in a higher operating temperature, which, according to the Carnot cycle, increases the engine's efficiency.

The battery packs in the aircraft are modular, meaning they will be able to be taken out of the fuselage after flight for charging. This is to eliminate the need of having to take the entire aircraft to a separate charging station after a flight to recharge before being able to fly again. With our system having modular batteries, the airports would be able to charge the batteries on the ground while the aircraft is in flight. Upon landing, a charged battery pack will already be available on the tarmac, depleted batteries would be exchanged with new ones, allowing the aircraft to return to flight instantly. The turnaround time for our system depends solely on the fueling time and speed at which the crew can replace the battery packs.

[3] "Engineus™ Smart Electric Motors." *Safran*, https://www.safran-group.com/products-services/engineustm.
[4] "Aircraft Database - PT6A-11AG Engine Model." Aircraft Database, https://aircraft-database.com/database/engine-models/pt6a-11ag.

Wing Airfoil Selections

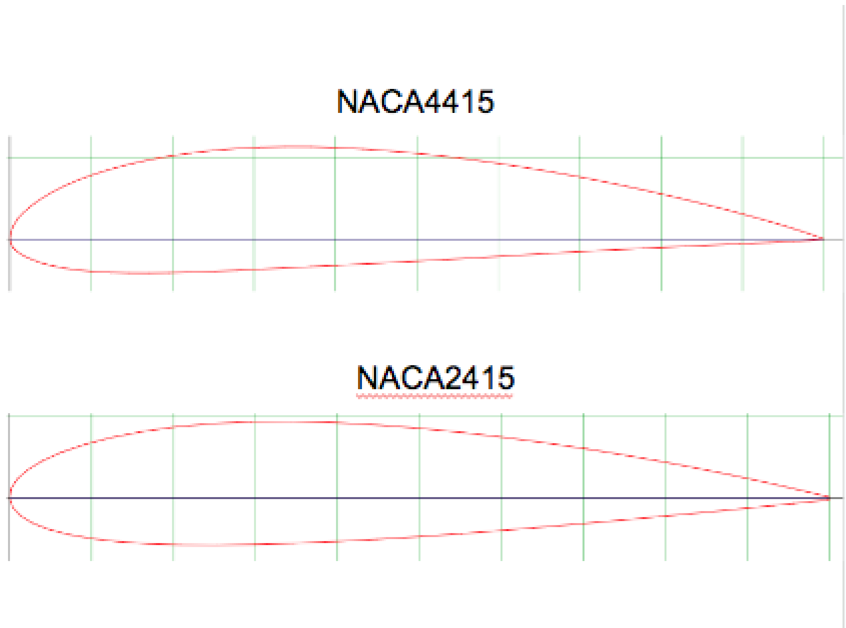

NACA 4415 and 2415. **Figure XII**

Wing Characteristics:

Root Chord: 6ft NACA4415
Tip Chord: 2.5ft NACA2415
L/D: 28 (just wing)
Length: 35ft
Wing area: 17.05m^2
Wetted area: 20.14m^2

The airfoil selection was done through trial and error in both SolidWorks and MatLab code to find a balance between lift and drag. The chosen design for the aircraft involves transitioning from a NACA4415 airfoil at the root to a NACA2415 airfoil at the middle of the wing. The implementation of a NACA4415 airfoil at the root with an angle of attack of 4 degrees transitioning to NACA2415 at 2.5 degrees at the middle, and then down to 1 degree at the tip, ensures the root will stall before the tip. A twist of 3 degrees was chosen for the aircraft as it is a

[5] "Airfoil Plot NACA2415." *NACA 2415 (n2415-IL)*, http://airfoiltools.com/airfoil/details?airfoil=n2415-il.

"Airfoil Plot NACA4415." *NACA 4415 (NACA4415-IL)*, http://airfoiltools.com/airfoil/details?airfoil=naca4415-il.

known standard used in aircraft design [6]. Also, having a higher camber at the root is necessary to produce the lift needed during flight while the low camber wing tip is necessary to control stalling. The NACA4415 airfoil has a 6 foot chord length from the root to the middle of the wing, which spans 17.5 feet. A 3 foot transition is then made to the NACA2415 airfoil, after which the chord length tapers from 6 feet to 2.5 feet, linearly decreasing for the rest of the span.

The simpler NACA 4 digit series was chosen over the newer higher camber wings to reduce the overall drag on the wing. The NACA wings selected are semi-symmetric meaning they will produce less drag while still producing adequate lift. Since the aircraft will not experience any weight loss during the ascent up to cruise, it was necessary to design the wing to produce enough lift with the maximum takeoff weight in mind. This is to ensure that the aircraft will be able to maintain straight and level flight during cruise. Also, the wing achieves a lift to drag ratio (L/D) of 28 which was achieved through our matlab calculations, and this result is supported by our SolidWorks flow simulation CFD.

Tail Geometry

The vertical and horizontal tail required for this aircraft may be smaller than those needed for a conventional long tube aircraft. The size of the tail was initially determined using equations 15 and 16 in Appendix A, which were derived from the Aircraft Design: A Conceptual Approach textbook by Raymer. The coefficients for these equations were assumed using values from the textbook for a twin turboprop aircraft since this type of aircraft has similar characteristics to what is being designed. In addition, it was estimated that the tail would be roughly 30 ft away from the quarter chord of the wing.

After designing the CAD model of the aircraft, the actual tail location was determined to be 10 ft closer than what was calculated. The wing was scaled down to a factor of .75 in height to compensate for this. However, despite the adjustment in size it still leaves the tail slightly oversized in the event of an engine-out scenario. The worst-case engine out scenario would be during the climb segment, losing all three electric motors on one wing. While a smaller tail could be used, it was decided to leave the tail slightly larger to ensure adequate control in the unlikely event of an engine-out scenario. If an engine out scenario were to occur during cruise, then the plane can transition over to its electric engines since it is a single turboprop engine.

[6] Raymer, Daniel P. *Aircraft Design: A Conceptual Approach*. American Institute of Aeronautics and Astronautics, 2018.

Force Calculations

For all the calculations of the wings, a MatLab code was developed that can be found in Appendix B, while all the equations used can be found in Appendix A. The lift of the wing was calculated by implementing equation 1 within a loop that integrated from the root to the tip of the wing, as the angle of attack, chord length, and coefficient of lift (Cl) changed. The Cl slopes can be found in Appendix C. For cruise conditions, straight and level flight, the lift needs to be equal to the weight. During the calculations, we obtained a lift value that was approximately equal to the weight, this was done by setting the cruise velocity to 185 knots. The density and temperature of air at 7.6 km is 0.54 kg/m^3 and 238.68K respectively. We opted for a slower cruise velocity in order to increase L/D ratio and the efficiency of the aircraft because of the non-retractable landing gear. The lift calculated was 18702.23 lbf or 83191.66 N and the L/D ratio for the wing is roughly 28. The drag was found using a combination of equations 2, 3, 4, and 14, which provided the drag of the wing plus the parasitic drag and the correction factor. The total drag is equal to 653.94 lbf or 2908.87 N. For takeoff conditions, we added a slotted flap, which can be seen in *Figure I* and *Figure II,* that shows a 15-degree flap used for takeoff conditions. Landing does not require as much lift force as take off, therefore the assumption can be made that slotted flaps increase the lift coefficient (Cl) by 1.3. We then take 60-80% of this value and recalculate the lift using the revised Cl [5]. Final calculated value for lift on takeoff is 19237.74 lbf or 85573.73 N.

Equations 5 and 6 were used to derive the cruise thrust. With knowledge of the aircraft's cruise velocity, propeller length, and propeller efficiency, we can calculate the exit velocity of air that passes through the propellers. The efficiency of the propeller is assumed to be 80% based on assumptions found for prop aircraft2. After determining the exit velocity, we substituted all the relevant values into equation 5 for the thrust power needed to maintain flight. The cruise thrust needed to maintain flight is 838.34 lbf or 3729.12 N. To determine the climb thrust required, we utilized equation 7 as outlined in the Raymer textbook. To calculate the climb thrust, we had to make an assumption about the climb L/D as the exact angle of attack for the climb was unknown. We decided to assume an angle of attack of approximately 5 degrees, as this typically yields the highest L/D ratio. The thrust required for climb was calculated to be 2365.36 lbf or 10521.65 N.

SolidWorks simulation

Displayed in *Figure III* and *Figure IV* is the wing bending stress on the root on the wing and the wing tip displacement respectively. These values were obtained through a SolidWorks force simulation in which the fuselage area remained fixed and the lift force acting on the wings was directed straight upwards. In *Figure III,* the maximum stress shown by the simulation is

83,400,000 N, which may be a significant amount of stress concentrated on an area of a wing, but it is feasible given our chosen material. We selected the 6061 T-6 aluminum alloy due to its lightweight nature, as well as its impressive tensile strength considering its low weight. The maximum stress before fatigue of aluminum 6061 T-6 is 289,579,806.31 N, which is well above the stress shown in the simulation[7]. As for the displacement in *Figure IV*, it may appear that the wing is bending in half but this is just an exaggeration. The wing only deflects about 7 inches at the wing tip, which is not substantial compared to the thickness of the root chord, which is also about 7 inches. This deflection will also decrease as the flight goes on and weight is dissipated from fuel burn also putting less stress on the wings.

In *Figure VI,* the comparison of pressure fields around the attachment from the wing root to the fuselage of the aircraft is shown. What we are observing is a pressure field that is more spread out for the version with a fillet. For the version with no fillet, there is more of a direct pressure point at the transition from wing to fuselage. In these contours, the plots go from red as the highest pressure down to blue as the lowest pressure. On the top of the wing near the root, there is an area of light blue which indicates a lower pressure. Essentially, what this means is that by incorporating a filet in the transition from the wing to the fuselage, the wing's lift is increased to a significant degree. This is reflected in the pressure surface contour visualization

Figure VII shows the flow trajectories over the wing at the root-fuselage intersection. What is displayed is what is expected from observing the pressure contour in *Figure VI,* the highest velocity is observed on the top of the wing, precisely at the point where the pressure is the lowest; this signifies the presence of lift.. For the velocity trajectory lines, the orange indicates higher velocity while the green indicates slower velocity, and yellow is in between. What we notice when comparing the two trajectories, which are fillet and no fillet, is that the wing with a fillet has a higher velocity over the wing shown by the darker orange trajectory lines. This is the second indication that the wing with a fillet at the intersection will increase lift and reduce drag on the overall wing.

As for the tail shown in *Figure V*, the pressure plot indicates there is a lower pressure going around the curve to the back of the tail, and once it gets to the trailing edge the pressure increases. This is typical for the shape we chose for the tail, we expect to see an increase in pressure where there is flow mixing from the different shaped structures. This could come from both separation of flow reattaching and also mixing in the trailing edge from the two sides of the tail.

The motors were assumed to weigh about 200 lbf each, this also takes in account the weight of the propeller and shroud surrounding the motor. With this, we were able to do a

[7] Cavallo, Christian. “All About 6061 Aluminum (Properties, Strength and Uses).” *Thomasnet® - Product Sourcing and Supplier Discovery Platform - Find North American Manufacturers, Suppliers and Industrial Companies*, https://www.thomasnet.com/articles/metals-metal-products/6061-aluminum/.

simulation for displacement in SolidWorks shown in *Figure IX*. The weight of the motors was barely able to bend the wing and at its peak displacement the wing only bends roughly 5mm. This will slightly mitigate the bending caused by the lift force during flight.

The full-plane CFD simulation for pressure, shown in *Figure XI* appears to align with our expectations. There is a pressure increase at all forward-facing edges, such as the front edge of the wings and the front of the tail. There is a pressure drop on top of the wing where the air speeds up and there is a corresponding pressure increase below the wing where there is a decrease in velocity. For the body of the aircraft, we expect some increase in pressure due to skin friction causing drag and slowing velocity on the sides of the aircraft.

Weight and Balance and Location of Major Components

The weight and balance for the plane were completed through an iterative process. After the chord of the wing at the root was determined, a center section of the fuselage was made. Next a forward and aft section were created, the sum of the length of these three sections is the length of the cargo area. The forward and aft sections were made such that they could be modified in length to move the center of gravity to the quarter chord of the wing. The cockpit and tailpieces were added to the ends of this cargo hold area to complete the entire fuselage structure. The PT6 is placed in the nose of the aircraft, so the only components that could be moved around to help move the center of gravity were the battery packs. Luckily, the center of gravity of the plane with the PT6 engine was still behind the quarter chord, therefore the battery packs were placed in front of the wings. The center of gravity of the aircraft sits halfway between the quarter and mid-chord. This will keep the aircraft at a slightly positive angle of attack during flight.

The batteries are positioned forward of the wing on the belly of the fuselage so that they can be easily interchanged. Each motor requires 220 lbs of batteries to operate. For six motors with an assumed weight of 80 lbs for the components to hold the battery pack together, the estimated battery pack weight is 1400 lbs. The fuel tanks are located inside the wings like many other conventional propulsion aircraft. In order to place electric motors on the wings, the turboprop engine was moved to the nose of the aircraft. This model of PT6 turboprop weighs 340 lbs. These main components and their placement can be seen in *Figure XIII* and *XIV* below. Weight and balance tables in Appendix B were made taking the moment about the leading edge of the wings.

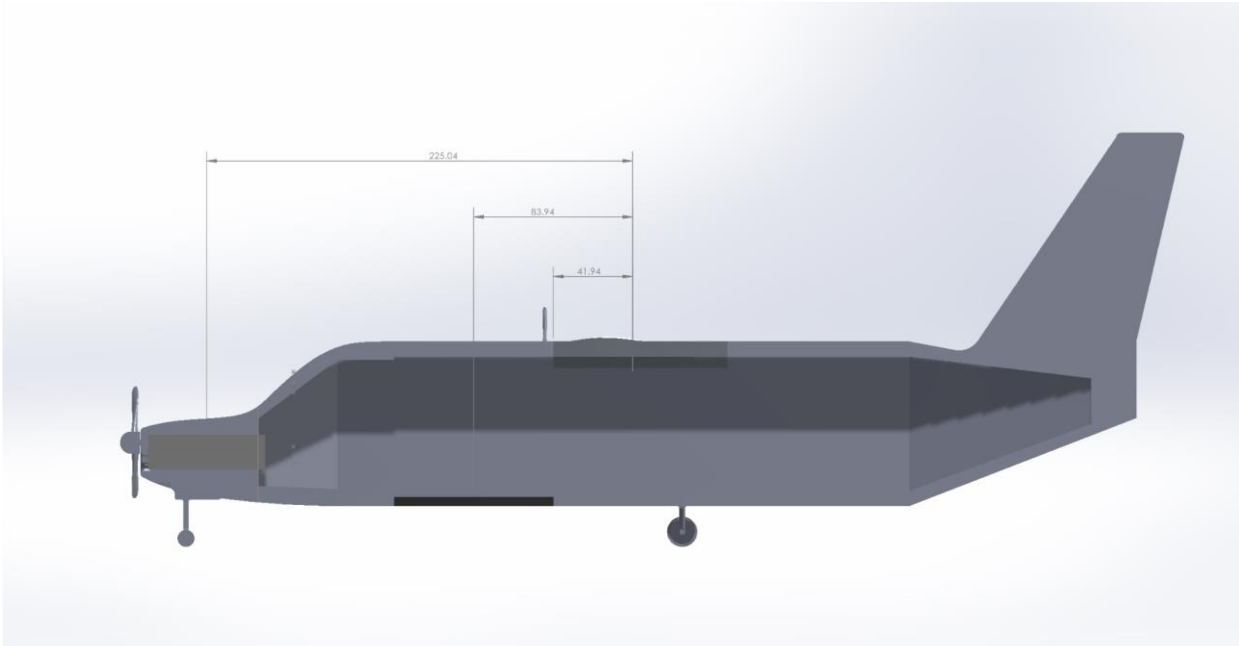

Major Components Distance From Center of Gravity in inches. **Figure XIII**

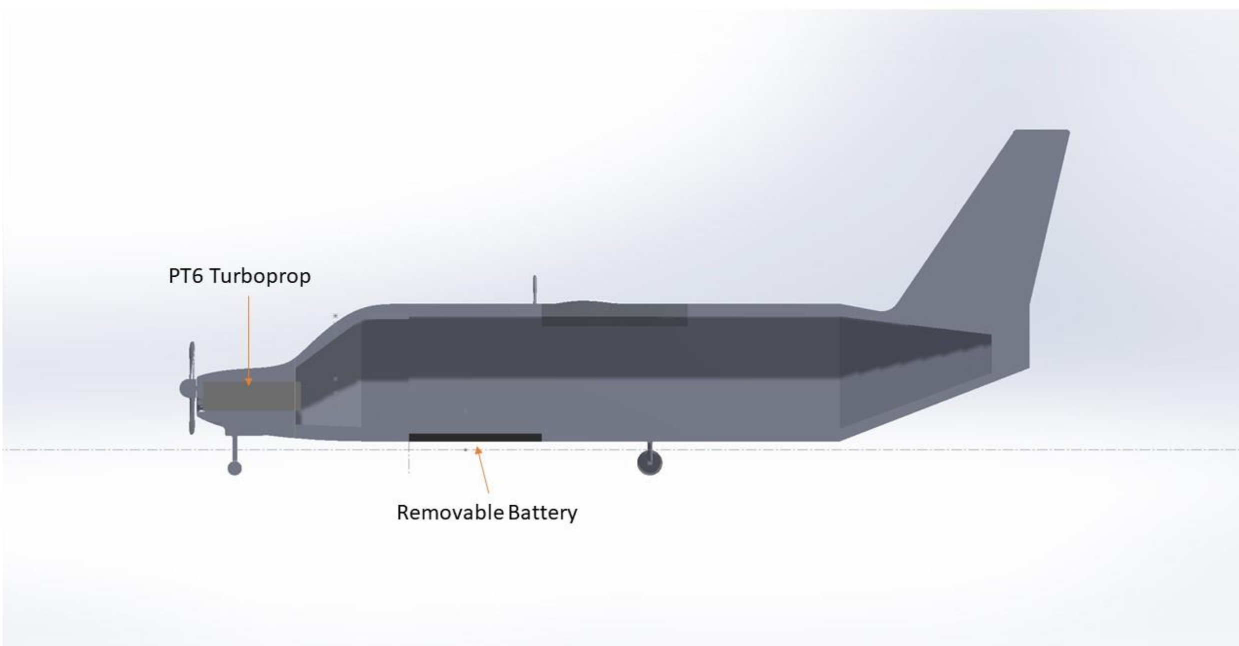

Interior Components. **Figure XIV**

References:

"Aircraft Database - PT6A-11AG Engine Model." Aircraft Database, https://aircraft-database.com/database/engine-models/pt6a-11ag.

"Airfoil Plot NACA2415." *NACA 2415 (n2415-IL)*, http://airfoiltools.com/airfoil/details?airfoil=n2415-il.

"Airfoil Plot NACA4415." *NACA 4415 (NACA4415-IL)*, http://airfoiltools.com/airfoil/details?airfoil=naca4415-il.

Cavallo, Christian. "All About 6061 Aluminum (Properties, Strength and Uses)." *Thomasnet® - Product Sourcing and Supplier Discovery Platform - Find North American Manufacturers, Suppliers and Industrial Companies*, https://www.thomasnet.com/articles/metals-metal-products/6061-aluminum/.

"Engineus™ Smart Electric Motors." *Safran*, https://www.safran-group.com/products-services/engineustm.

Raymer, Daniel P. *Aircraft Design: A Conceptual Approach*. American Institute of Aeronautics and Astronautics, 2018.

Appendix A

[1] $L = 0.5*Rho*V^2*S*Cl$ (Lift)
[2] $D = 0.5*Rho*V^2*S*Cd$ (drag)
[3] $e = 1.78*(1-0.045*AR^{0.68})-0.64$ (Oswald efficiency factor)
[4] k = 1/(pi*e*AR) (Drag correction factor)
[5] Pt = rho*v*s*(v-vo) (Thrust power)
[6] v = ((2/n)-1)*vo (exit velocity leaving a propeller)
[7] TWclimb = (1/ldclimb)+(Vert/V) (Thrust/Weight for climb)
[8] $Vs = sqrt((2*w)/(Cl_{max}*rho*s))$ (stall velocity)
[9] $Lambda = C_{tip}/C_{root}$ (Taper)
[10] S = L*MAC (Wing area)
[11] $MAC=(2/3)*Cbig*(1+lambda+lambda^2)/(1+lambda)$ (Mean aerodynamic chord)
[12] Cl2415 = (41/400)*AoA + 0.25 (Cl for 2415 slope)
[13] Cl4415_noFlap = (43/500)*AoA+0.65 (Cl for 4415 slope, no flap)
[14] $Cdo = K*ClAvg^2-Cd$ (parasitic Cd)
[15] S_VT = (C_VT*b_w*S_w)/L_VT (Area of Vertical Tail)
[16] S_HT = (C_VT*MAC_w*S_w)/L_HT (Area of Horizontal Tail)

Appendix B

```
clear;
clc;

%Chord lineraly decreasing from root to tip
C_root = 6/3.281; %m
C_tip = 2.5/3.281; %m
span = 70/3.281; % m
Uinfknots = 185; %knots
Uinf = Uinfknots/1.944; %mps
W = 19000/2.205;
rho = 0.549; %kg/m^3 density of air at 25000ft (cruise altitude)
b = span/2;
AoAmaxRoot = 15; %degrees
AoAmaxTip = 17;
%%%% FULL WING CALCULATIONS %%%%

%Taper
lambda = lambdaf(C_tip,C_root);

%MACCho
MACfullWing = MAC(lambda,C_root);

%wing area
S = Sf(b,MACfullWing);


%%%% SPAN DIVISION %%%%


%MAC of root to mid
%Enter bigger section of wing you are calculating
MACrm = C_root;
%MAC from mid to tip
MACmt = MAC(lambda,C_root);
MACavg = (MACrm+MACmt)/2;


%Wing area of root to the middle of wing and middle of the wing to tip
L1 = b/2; %m %Length from root to mid
L2 = L1; %M %Length from mid to tip
S_rm = Ss(MACrm,L2);
```

```
S_mt = Ss(MACmt,L2);
S_tot = S_mt+S_rm;

%From solid works
S_Wetted = 20.14; %m^2


%%%% LIFT CALCULATIONS %%%%
%%%% NO FLAPS %%%%

%AoA is approximately linearly decreasing from root to tip

%Cl from slope of Cl vs AoA curve (4 deg at root 1 deg at tip)
CL3 = Cl4415_noFlap(4);
CL15 = Cl4415_noFlap(2.5);
Cl15 = Cl2415(2.5);
Cl0 = Cl2415(1);

%From slopes
lr = LiftNoFlap(rho,Uinf,MACrm,CL15,CL3);
lt = LiftNoFlap(rho,Uinf,MACmt,Cl0,Cl15);
ltot = lr+lt; %newton
lbf = ltot*0.224809; %newton to lbf

fprintf("Cruise")
fprintf("\nlift of one wing is %.2flbf or %.2fN.",lbf,ltot)

lift_both_wings = lbf*2;
fprintf("\nLift of both wings is %.2flbf.",lift_both_wings)

%%%% WITH FLAPS FOR TAKEOFF %%%%

%Approximation from table 12.2 slotted flaps with takeoff conditions

lr_flapped = lr*1.3*0.8;
ltot_flapped = lr_flapped+lt;
fprintf("\n\nTakeoff")
fprintf("\nFlapped wing gives %.2fN lift.",ltot_flapped)

ltot_flapped_lbf = ltot_flapped/4.448*2;
fprintf("\nTakeoff lift is %.2flbf.",ltot_flapped_lbf)
```

```
%%%% WITH 60 DEGREE FLAPS FOR LANDING %%%%
Amin = 1;
Amax = 4;
UinfLand = 80; %knots
UinfLanding = UinfLand/1.944; %mps

Lflapped60R = flap60(rho,UinfLanding,S_rm,Amin,Amax);
LflappedT = Lflapped60R+lt;
LflappedTlb = LflappedT/4.448;
fprintf("\n\nLanding")
fprintf("\nLift with 60 degree flaps at the same AoA as cruise is %.2flbf",LflappedTlb)


%%%% OTHER %%%%
%Stall velocity (cruise)
ClmaxRoot = Cl4415_noFlap(AoAmaxRoot);
ClmaxTip = Cl2415(AoAmaxTip);
VsRoot = vs(W,ClmaxRoot,rho,S_tot);
VsTip = vs(W,ClmaxTip,rho,S_tot);
Vs = (VsRoot+VsTip)/2;
%Root and rip are roughly the same stall velocity. I will use 30m/s
Vto = 1.1*Vs; %Needs to be greater than or equal to this
Vcl = 1.2*Vs; %Needs to be greater than or equal to this

AR = b/MACavg;
K = k(AR);

D1wing = 0.5*rho*(Uinf^2)*S_tot*0.009;

T_cruise = 0.1*W;

ClAvg = (Cl0+Cl15+CL15+CL3)/4;
Cd = 0.009;

Cdo = K*ClAvg^2-Cd;
Do = 0.5*rho*Uinf^2*60*Cdo;
Drag_tot = (Do+D1wing)/4.448; %lbf

LDcruise = lift_both_wings/Drag_tot;
fprintf("\nLD for cruise is %.2f.",LDcruise)

%for cruise
n = 0.8; %Propeller propulsive efficiency based on a typical v/vo = 1.5
dp = 1; %propeller diameter m
```

```
Pthrust = Pt(rho,dp,Uinf,n);
Pthrustlb = Pthrust/4.448;
fprintf("\n\nThrust needed for cruise V is %.2flbf.",Pthrustlb)
%for climb
Vert = 5.08; %m/s
%ldmax = 120; %comes from cl/cd vs alpha curve on airfoiltools.com at 5 deg AoA


Tclimb_ = TWclimb(120,Vert,Uinf)*(W*4.448);
fprintf("\nFor climb thrust needs to be %.2flbf.",Tclimb_)





%%%% FUNCTIONS %%%%

%4415(no flap) slope for cl from Airfoltools.com
function [Cl4415_noFlap] = Cl4415_noFlap(AoA)
   Cl4415_noFlap = (43/500)*AoA+0.65;
end

%2415 slope for cl from Airfoltools.com
function [Cl2415] = Cl2415(AoA)
   Cl2415 = (41/400)*AoA + 0.25;
end

%Lift with flap
function [LiftFlap] = LiftFlap(rho,Uinf,S,Cl_min,Cl_max)
   Cl = Cl_max;
   LiftFlap = 0;
   while Cl > Cl_min
      LiftFlap = LiftFlap + 0.5*rho*(Uinf^2)*S*Cl;
      Cl = Cl-0.02;
   end
end

%60 degree flap
function [flap60] = flap60(rho,uinf,s,AoAmin,AoAmax)
   clmax = (1/10)*AoAmax+1.9;
   clmin = (1/10)*AoAmin+1.9;
   cl = clmax;
   flap60 = 0;
   while cl > clmin
```

```
        flap60 = flap60 + 0.5*rho*(uinf^2)*s*cl;
        cl = cl-0.02;

    end
end

%lift with no flap
function [LiftNoFlap] = LiftNoFlap(rho,Uinf,S,Cl_min,Cl_max)
    Cl = Cl_max;
    LiftNoFlap = 0;
    while Cl > Cl_min
        LiftNoFlap = LiftNoFlap + 0.5*rho*(Uinf^2)*S*Cl;
        Cl = Cl-0.02;
    end
end

%Mean Aerodynamic Chord function
function [MAC] = MAC(lambda,Cbig)
    MAC = (2/3)*Cbig*(1+lambda+lambda^2)/(1+lambda);
end

%S function for full wing
function [Sf] = Sf(b,MAC_FullWing)
    Sf = b*MAC_FullWing;
end

%S function for wing segments
function [Ss] = Ss(MAC_WingSection,L)
    Ss = L*MAC_WingSection;
end

%lambda function
function [lambdaf] = lambdaf(Csmall,Cbig)
    lambdaf = Csmall/Cbig;
end

function [vs] = vs(w,clmax,rho,s)
    vs = sqrt((2*w)/(clmax*rho*s));
end

function [drag4415] = drag4415(rho,v,s,Cd_min,Cd_max)
    cd = Cd_max;
    DragNoFlap = 0;
    while cd > Cd_min
```

```
        DragNoFlap = DragNoFlap + 0.5*rho*(v^2)*s*cd;
        cd = cd-0.02;
    end
end




%induced drag correction factor
function [k] = k(AR)
    e = 1.78*(1-0.045*AR^0.68)-0.64;
    k = 1/(pi*e*AR);
end

function [Pt] = Pt(rho,s,vo,n) %S is diameter of propellers
    v = ((2/n)-1)*vo;
    Pt = rho*v*s*(v-vo); %Newtons
end

function [TWclimb] = TWclimb(ldclimb,Vert,V) %Vert is vertical climb rate
    TWclimb = (1/ldclimb)+(Vert/V);
end
```

Appendix C

NACA4415 plots(airfoilplots.com)

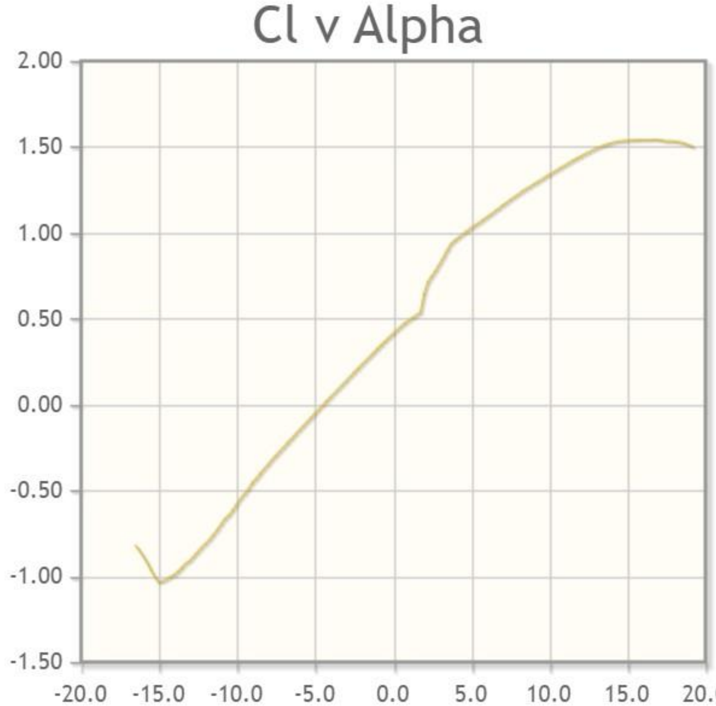

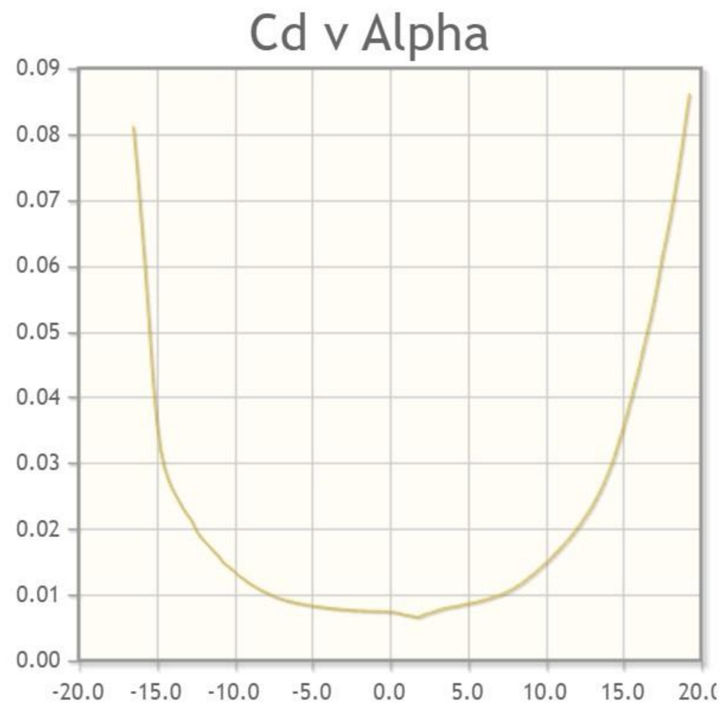

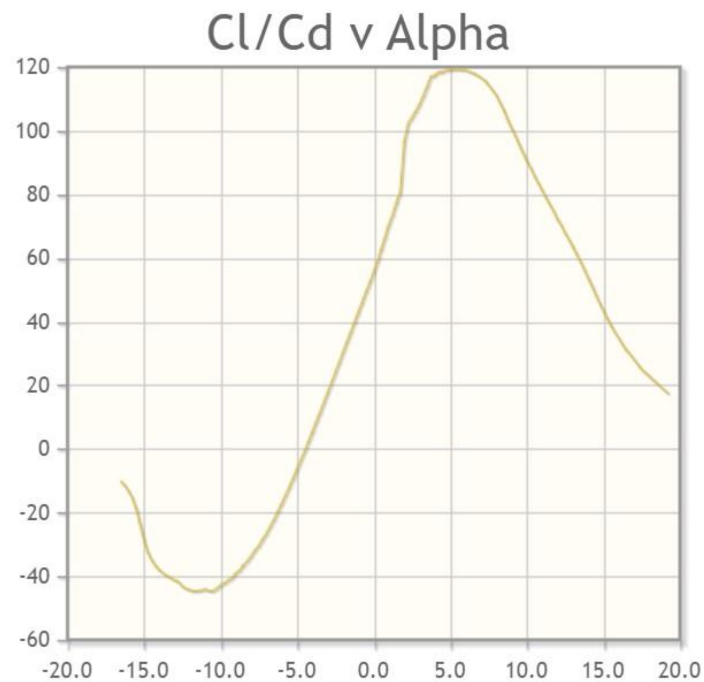

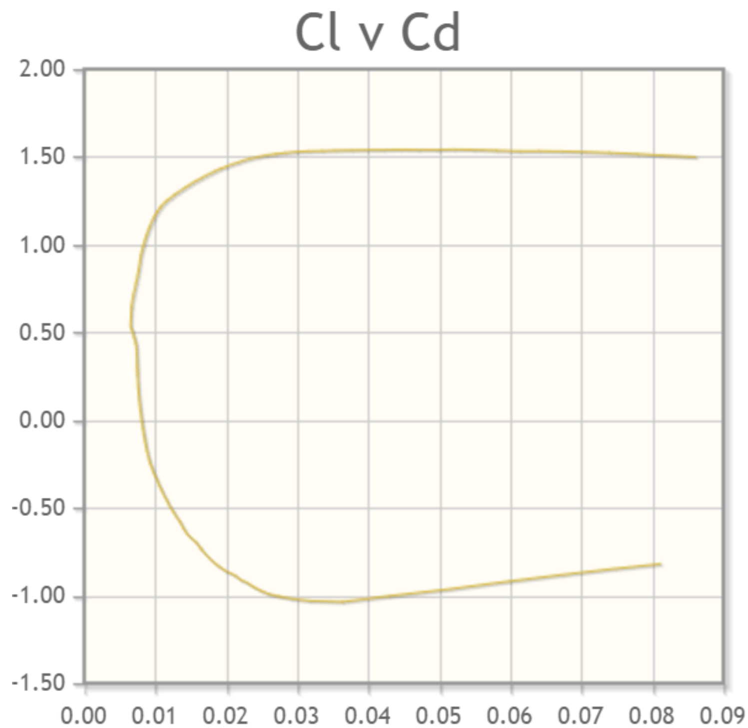

NACA2415(airfoilplots.com)

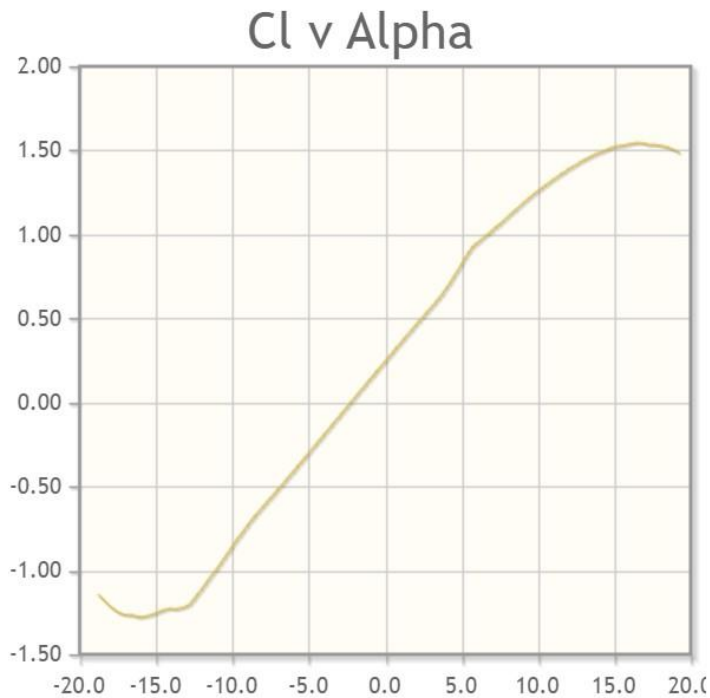
Cl v Alpha
2.00
1.50
1.00
0.50
0.00
-0.50
-1.00
-1.50
-20.0
-15.0
-10.0
-5.0
0.0
5.0
10.0
15.0
20.(

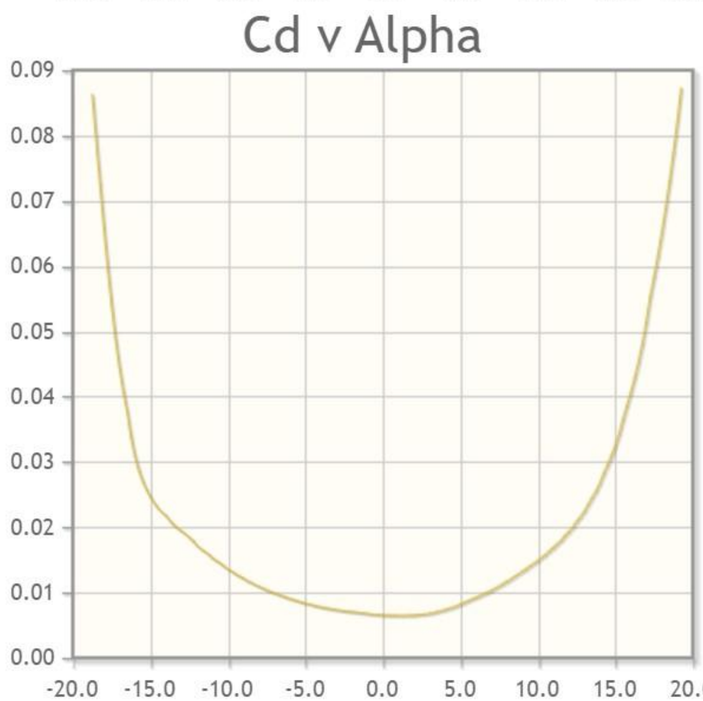
Cd v Alpha
0.09
0.08
0.07
0.06
0.05
0.04
0.03
0.02
0.01
0.00
-20.0
-15.0
-10.0
-5.0
0.0
5.0
10.0
15.0
20.(

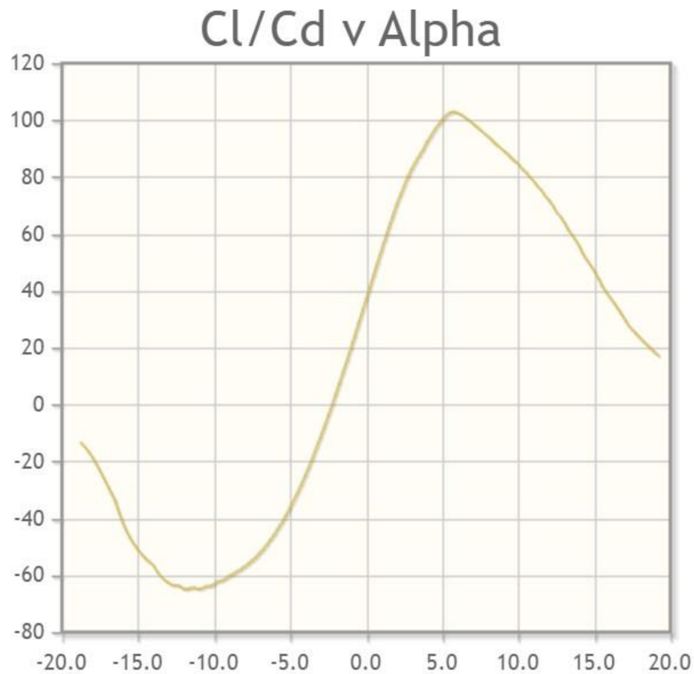
Cl/Cd v Alpha
120
100
80
60
40
20
0
-20
-40
-60
-80
-20.0
-15.0
-10.0
-5.0
0.0
5.0
10.0
15.0
20.0

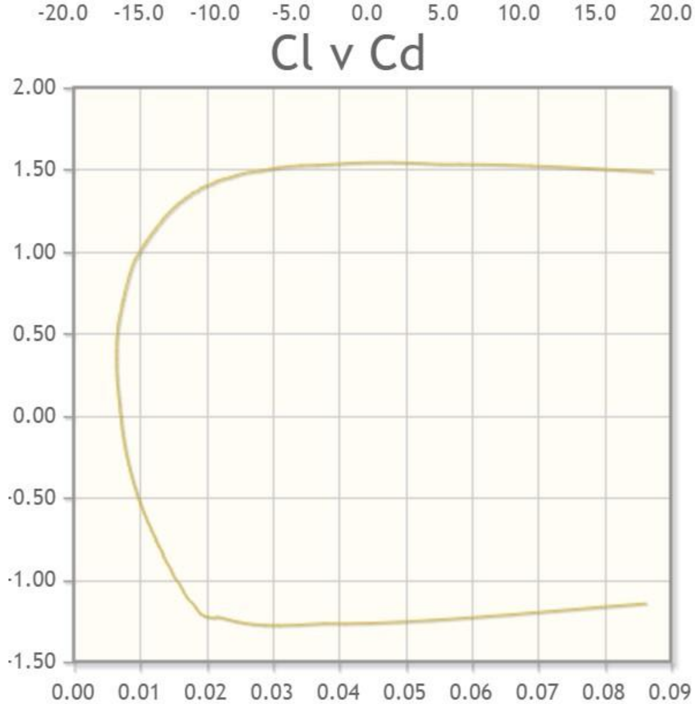
Cl v Cd
2.00
1.50
1.00
0.50
0.00
-0.50
-1.00
-1.50
0.00
0.01
0.02
0.03
0.04
0.05
0.06
0.07
0.08
0.09

Appendix D

Project Weight and Balance

April 27, 2023

[6]:
```
pip install tabulate
```

```
Collecting tabulate
  Using cached tabulate-0.9.0-py3-none-any.whl (35 kB)
Installing collected packages: tabulate
Successfully installed tabulate-0.9.0
WARNING: You are using pip version 21.2.4; however, version 23.1.2 is
available.
You should consider upgrading via the '/opt/conda/bin/python -m pip install
--upgrade pip' command.
Note: you may need to restart the kernel to use updated packages.
```

[7]:
```
from tabulate import tabulate
```

All measurements taken in reference to wing leading edge

[8]:
```
w_ac = 13725 # aircraft weight (lbs)
r_pilots = 120.33 # distance to pilots (in)
w_pilots = 400 # weight pilots (lbs)
```

[9]:
```
def radius_cg(m, r):
    '''
    inputs
    m - mass
    r - distance from leading edge (positive is toward front of plane)

    returns:
    r_cg - distance from leading edge
    '''
    r_cg = (-(m*r)-(r_pilots*w_pilots)) / w_ac
    return(r_cg)
```

[10]:
```
# empty weight CG calc
m_empty = 0
r_empty = 0
r_cg_empty = radius_cg(m_empty, r_empty)
```

1

```
print(r_cg_empty, "in")
```

```
-3.5068852459016395 in
```

[11]:
```
# max weight calc assuming load takes full cargo space and load CG is at␣
↪geometric center of load
m_max = 4409
r_max = -43.6
r_cg_max = radius_cg(m_max, r_max)
print(r_cg_max, "in")
```

```
10.49911839708561 in
```

[12]:
```
# half weigh calc, load is located at CG of batteries
m_half = 4409/2
r_half = 42
r_cg_half = radius_cg(m_half, r_half)
print(r_cg_half, "in")
```

```
-10.252896174863388 in
```

[14]:
```
# half weight at tailing edge of wing
m_te = 4409/2
r_te = -92
r_cg_te = radius_cg(m_te, r_te)
print(r_cg_te, "in")
```

```
11.270091074681238 in
```

[15]:
```
data = [[m_empty, r_empty, r_cg_empty], [m_max, r_max, r_cg_max], [m_half,␣
↪r_half, r_cg_half], [m_te, r_te, r_cg_te]]
col_names = ['Weight', 'Radius From Leading Edge', 'CG Distance From Leading␣
↪Edge']

print(tabulate(data, headers = col_names))
```

```
  Weight    Radius From Leading Edge    CG Distance From Leading Edge
--------  --------------------------  -------------------------------
     0                           0                           -3.50689
  4409                       -43.6                           10.4991
  2204.5                      42                            -10.2529
  2204.5                     -92                             11.2701
```

[ ]:

Appendix E